Quantification of Colloid Retention and Release by Straining and Energy Minima in Variably Saturated Porous Media

ARTICLE *in* ENVIRONMENTAL SCIENCE & TECHNOLOGY · JUNE 2013

Impact Factor: 5.33 · DOI: 10.1021/es400288c · Source: PubMed

8 AUTHORS, INCLUDING:

Wenjing Sang
Tongji University
10 PUBLICATIONS **105** CITATIONS
SEE PROFILE

Verónica L Morales
ETH Zurich
22 PUBLICATIONS **391** CITATIONS
SEE PROFILE

Cathelijne Stoof
Wageningen University
49 PUBLICATIONS **241** CITATIONS
SEE PROFILE

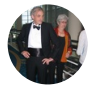

Tammo S Steenhuis
Cornell University
646 PUBLICATIONS **10,331** CITATIONS
SEE PROFILE

Environmental Science & Technology

Article

pubs.acs.org/est

Quantification of Colloid Retention and Release by Straining and Energy Minima in Variably Saturated Porous Media

Wenjing Sang,[†,‡,§] Verónica L. Morales,[∥] Wei Zhang,[⊥] Cathelijne R. Stoof,[‡] Bin Gao,[#] Anna Lottie Schatz,[‡] Yalei Zhang,[§,*] and Tammo S. Steenhuis[‡,*]

[†]National Engineering Research Center for Facilities Agriculture, Institute of Modern Agricultural Science and Engineering, Tongji University, Shanghai 200092, China

[‡]Department of Biological and Environmental Engineering, Cornell University, Ithaca, New York 14853, United States

[§]State Key Laboratory of Pollution Control and Resources Reuse, College of Environmental Science and Engineering, Tongji University, Shanghai 200092, China

[∥]SIMBIOS Centre, University of Abertay Dundee, Bell Street, Dundee, DD1 1HG, Scotland

[⊥]Department of Plant, Soil and Microbial Sciences, Environmental Science and Policy Program, Michigan State University, East Lansing, Michigan 48824, United States

[#]Department of Agricultural and Biological Engineering, University of Florida, Gainesville, Florida 32611, United States

Supporting Information

ABSTRACT: The prediction of colloid transport in unsaturated porous media in the presence of large energy barrier is hampered by scant information of the proportional retention by straining and attractive interactions at surface energy minima. This study aims to fill this gap by performing saturated and unsaturated column experiments in which colloid pulses were added at various ionic strengths (ISs) from 0.1 to 50 mM. Subsequent flushing with deionized water released colloids held at the secondary minimum. Next, destruction of the column freed colloids held by straining. Colloids not recovered at the end of the experiment were quantified as retained at the primary minimum. Results showed that net colloid retention increased with IS and was independent of saturation degree under identical IS and Darcian velocity. Attachment rates were greater in unsaturated columns, despite an over 3-fold increase in pore water velocity relative to saturated columns, because additional retention at the readily available air-associated interfaces (e.g., the air−water−solid [AWS] interfaces) is highly efficient. Complementary visual data showed heavy retention at the AWS interfaces. Retention by secondary minima ranged between 8% and 46% as IS increased, and was greater for saturated conditions. Straining accounted for an average of 57% of the retained colloids with insignificant differences among the treatments. Finally, retention by primary minima ranged between 14% and 35% with increasing IS, and was greater for unsaturated conditions due to capillary pinning.

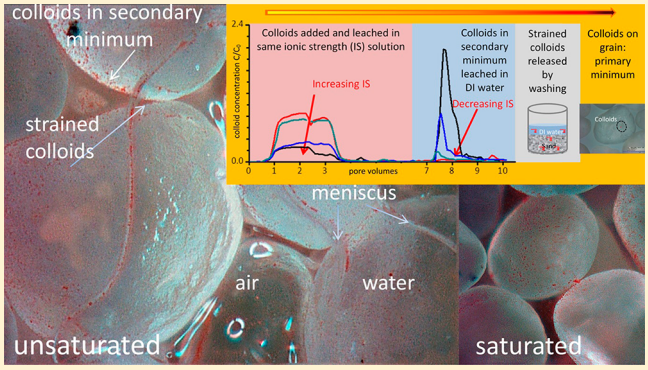

INTRODUCTION

Colloidal transport in porous media has gained notable attention over the past few decades as facilitated contaminant transport in groundwater aquifers, reduced permeability of oil and gas reservoirs, and in situ remediation strategies have become topics of concern in various fields.[1,2]

A large body of experimental and theoretical work has been carried out to understand key physicochemical factors affecting colloid transport and deposition in natural porous media. Solution composition has been extensively investigated with particular emphasis on ionic strength (IS)[3−5] and pH[5−8] for affecting electrostatic interactions, natural organic matter,[5,8] and surfactants as electrosteric stabilizers, and cation valence[8] in terms of neutralizing surface charge. Each of these factors affects surface interactions between colloids and between colloids and the porous medium's surface. In addition, unsaturated conditions significantly increase colloid retention by the presence of a gas phase, which restricts the geometry of the fluid phase and partitions deposited colloids toward interfaces that are absent in fully saturated media (e.g., air−water and air−water−solid interfaces).[9−15] Flow rate affects low-flow or flow-stagnation zones where colloids can become trapped.[3,15] Moreover, high flow velocities have been related to increased applied torque from strong hydrodynamic drag forces

Received: January 20, 2013
Revised: June 16, 2013
Accepted: June 27, 2013
Published: June 27, 2013

that can shear colloids associated with the medium's surface.[16−20]

Traditionally, colloid retention at the solid-water interface in both unsaturated and saturated porous media has been justified by energy profiles derived from DLVO theory. As such, irreversible retention is attributed to colloid attachment at chemically attractive microsites on naturally heterogeneous porous media surfaces by primary minimum interactions.[19,21−24] Reversible retention is attributed to weak association of colloids with the solid surface owing to secondary minimum interactions.[22,25−28]

Additional mechanisms of greater complexity are often implicated when classic DLVO interaction profiles do not agree with transport trends. In unsaturated media, retention in sites associated with the air phase is generally accepted. Colloid retention at the air−water interface (AWI)[29] or at wedge-shaped locations, where menisci become thin against media grains,[30] have been previously reported. Calculated capillary forces at this meniscus edge are estimated to be several orders greater than DLVO forces.[17,31,32] For media of any water saturation level, retention by pore straining is expected when colloid-collector size ratios are large,[33−38] and in regions of wedged pore space (e.g., grain-to-grain contacts, air−water−solid [AWS] interface wedges, and surface crevices), which are regions of low flow velocities where hydrochemical conditions are favorable[39,40] and DLVO interactions are attractive.[34,41,42] In this study we do not attempt to differentiate between the above listed types of straining, but rather investigate this retention mechanism as it is driven by structural restrictions.

Understanding processes responsible for re-entrainment of colloids into the bulk fluid by chemical perturbations has become a topic of high priority in the past few years. Colloid detachment kinetics has been investigated by many in saturated porous systems, where detachment processes are induced by changes in solution IS and pH.[3,4,13,18,22,26,28,43] The observed colloid detachment from such chemical perturbations has been attributed to the expansion of electric double layers and/or the increased magnitude of negative surface charge, which would increase the span and height of energy barriers, diminish secondary energy wells, and consequently release colloids retained by energy minima.

Despite the wealth of information available on the variety of mechanisms responsible for colloid retention and release, the relative contribution of each implicated mechanism toward deposition, even under simple steady-state conditions, remains elusive. This knowledge gap is particularly evident when deposition kinetics are extracted from breakthrough curves (BTCs) and deposition profiles, as these data amalgamate into one signal the effect of all deposition and re-entrainment processes. Therefore, the overall aim of this research is to elucidate the relative contribution of three key retention mechanisms of colloid transport and retention: (i) reversible secondary minima deposition, (ii) pore straining, and (iii) irreversible attachment by primary minima interactions. Toward this objective, column transport tests were performed by injecting synthetic colloids through sand-packed columns conditioned at a range of typical groundwater IS levels (i.e., 0.1, 1, 10, and 50 mM) under steady-state conditions for fully- and partially water saturated conditions. Colloid retention was first established for each IS level under hydrochemical steady-state. Second, solution IS reduction was used to elute colloids reversibly retained by secondary minima. Third, destructive sampling of the sand column provided the depth profile of colloids retained by pore straining. Fourth, mass balance calculations were used to estimate the fraction of injected colloids retained by irreversible primary minima attachment. Lastly, statistical analysis is presented for effects that initial IS and moisture content have on the relative contribution of each retention mechanism toward overall retention.

MATERIALS AND METHODS

Colloids and Porous Media. Carboxylated red-dyed polystyrene microspheres of 3 μm diameter (Polysciences, Inc., Warrington, PA) were used as model colloids. Prior to experimentation, the colloids were washed with deionized (DI) water to remove the manufacturer-added stabilizing surfactant. Surfactant-free colloids were dispersed at a concentration of 1.68×10^7 particles mL^{-1} in NaCl solutions at 0.1, 1, 10, or 50 mM IS and pH of 6. Additional colloid-free background NaCl solutions of matching IS were prepared, while DI water was used as the background solution of 0 mM IS.

Angular translucent quartz sand (AGSCO Corporation, Hasbrouck Heights, NJ) was sieved to a size range of 0.59−0.84 mm. Detailed chemical properties of the quartz sand are reported elsewhere.[15] The sand was acid-cleaned to remove surface impurities and minimize chemically attractive microsites on the sand, as described by Litton and Olson.[44]

Electrophoretic Mobility and Hydrodynamic Diameter Measurements. Sand fragments were created as per Kuznar and Elimelech[43] and dispersed in the background NaCl solutions. Electrophoretic mobility (EM) of the colloid and sand fragment suspensions was measured by the zetasizer (Nano-ZS, Malvern Instruments Ltd., Worcestershire, UK). The ζ-potentials at 0 mM IS was calculated from the EM values based on the table in Ottewill and Shaw,[45] and the ones at higher IS levels (0.1, 1, 10, or 50 mM) with models derived by O'Brien and Hunter.[46] Calculation details are reported in Supporting Information (SI) S1. Hydrodynamic diameter (D_h) of colloid suspensions at each IS tested was measured over a period of 60 min to examine colloid stability. Details of these measurements are reported in SI S1.

Colloid Retention and Release Experiments. The sand was wet-packed into a glass column of $1 \times 1 \times 20$ cm to a porosity of 0.40 cm^3 cm^{-3}. The bottom end of the column was fitted with a porous ceramic plate (40−50 μm pore size). The influent was added to the top of the column with a peristaltic pump at a flow rate (q) of 0.5 mL min^{-1} for all experiments. Water saturation was maintained throughout the experiments for saturated columns. To establish unsaturated conditions, a constant tension of −2.5 kPa was maintained at the bottom of the column using a hanging water column until a volumetric moisture content (θ_w) of 0.12 cm^3 cm^{-3} was achieved, as determined by the gravimetrical method. Pore-scale images were collected with bright field microscopy as per Morales et al.[14] throughout the transport experiments to obtain qualitative visual information about colloid retention sites. The experimental setup is schematically illustrated in SI Figure S2. Each transport experiment as described below was carried out in duplicate or triplicate.

Our transport experimental protocol is modified from earlier studies,[22,27,47] as illustrated in SI Figure S3. Prior to the transport experiments, the columns were conditioned by flushing 32 mL of DI water, followed by an additional 32 mL of colloid-free background NaCl solutions. Next, a pulse of the colloidal suspension was injected for 2.5 and 8.3 pore volumes (PVs) for saturated and unsaturated conditions, respectively,

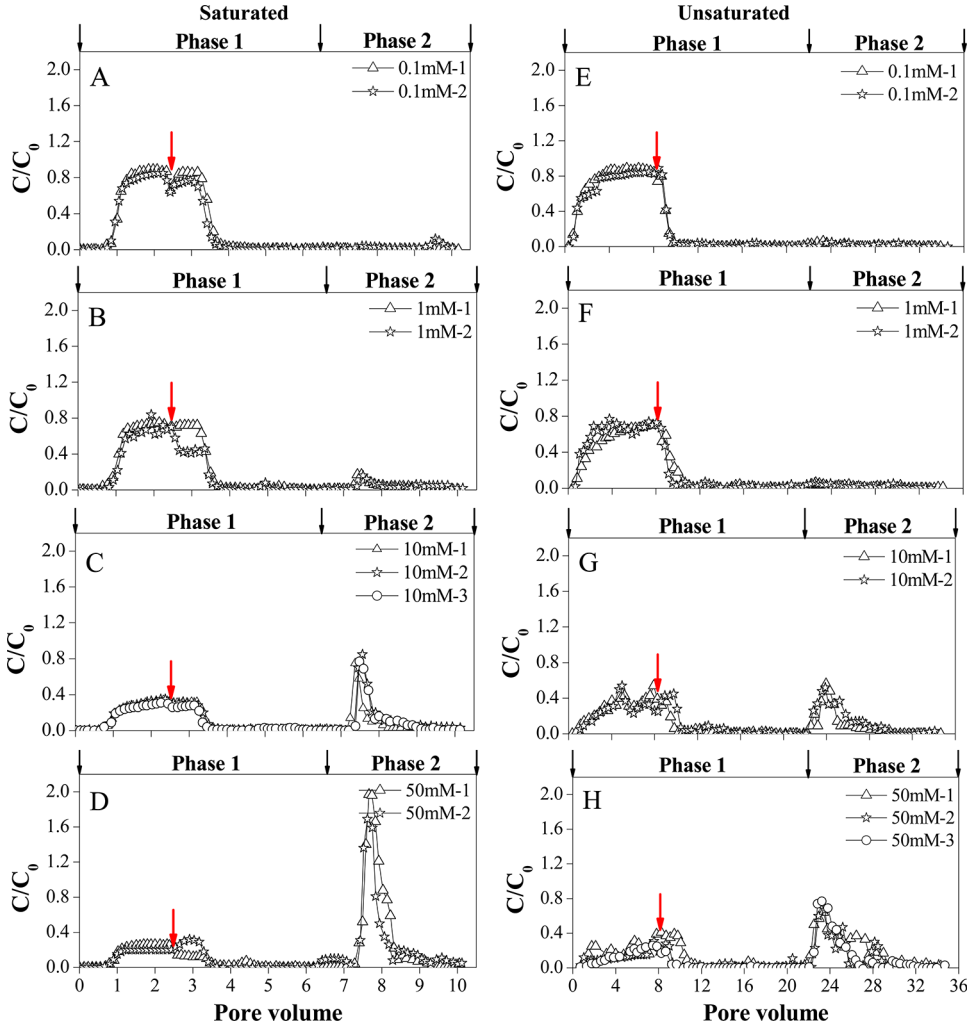

Figure 1. Effect of ionic strength on colloid deposition and release under unsaturated and saturated conditions. Phase 1: breakthrough curve (colloid retention); phase 2: elution with DI water (colloids release). A–D: saturated; E–H: unsaturated. Red arrows indicate the change of influent to colloid-free background solution.

followed by an injection of colloid-free background NaCl solution until the effluent colloid concentration was negligible (i.e., 4 and 13.3 PVs for saturated and unsaturated conditions, respectively). This experimental stage is referred to as phase 1 and corresponds to the first BTC in Figure 1, as shown in the Result section. At the end of phase 1, a second flush of colloid-free DI water was added for 4 and 13.3 PVs for saturated and unsaturated conditions, respectively. This experimental stage is referred to as phase 2 and corresponds to the second BTC in Figure 1. Additional data monitoring the changes in effluent chloride concentration during phase 2 (SI Figure S4) confirmed that the exchange of pore water from NaCl solution to DI water was efficient and followed plug-flow behavior. The column saturation degree remained constant between phase 1 and 2. Experiments were performed at initial IS of 0.1, 1, 10, or 50 mM under saturated and unsaturated conditions. The effluent colloid concentration was monitored in discrete samples using a spectrophotometer (Spectronic 501, Milton Roy, Ivyland, PA) at a wavelength of 550 nm. Colloid concentrations were employed within the linear range between absorbance and colloid concentration.

At the end of phase 2 (i.e., the elution of the second BTC), deposition profiles were obtained following a similar protocol from Bradford et al.,[35] here referred to as phase 3. Briefly, the sand was carefully removed from the column and segmented into 2- cm fractions. Each segment was immersed into 10 mL of DI and gently mixed to resuspend colloids that were retained due to soil pore structure, but not attached to the sand grains. The colloid concentration in the supernatant for each segment was measured and the colloids retained per unit sand mass reported as a function of column depth (i.e., colloid spatial deposition profiles). Values of retained colloids are reported as fraction of colloids from the total mass of colloids applied, W_T, and fraction of colloids from the total mass of retained particles in phase 1, W_R. Additional data pertaining fractions of colloids retained or recovered in each experiment are reported with the following systematic nomenclature. The symbol W is used to indicate the fraction of colloids suspended in the effluent, and M is used to indicate the fraction of colloids retained in the column. Subscript numbers (subscript 1, 2, or 3) indicate the experimental phase to which the data correspond, while subscript letters indicate whether the value is expressed as a fraction of the total colloids applied (subscript T) or the amount of colloids retained during phase 1 (subscript R).

Measured Retention Mechanisms. Hydrodynamic parameters for saturated and unsaturated conditions were determined via inverse fitting of BTCs of a conservative tracer (NaCl), for average pore-water velocities (v) and dispersion

Table 1. Comparison of Colloids Recovered during Transient Transport Experiments under Saturated and Unsaturated Conditions

		colloid recovery in effluent							
		phase 1	phase 2 (secondary minimum)		colloids recovered by column dissection (straining)		colloids not recovered (primary minimum)		colloids retained
	ionic strength during Phase 1 (IS, mM)	W_{T1}[a] (fraction of total applied)	W_{T2} (fraction of total applied)	W_{R2} (fraction of total retained)	W_{T3} (fraction of total applied)	W_{R3} (fraction of total retained)	M_{T3} (fraction of total applied)	M_{R3} (fraction of total retained)	M_{T1} (fraction of total applied)
unsaturated	0.1	0.78 ± 0.09	0.02 ± 0.01	0.10 ± 0.03	0.13 ± 0.06	0.59 ± 0.24	0.07 ± 0.06	0.30 ± 0.27	0.22 ± 0.01
	1	0.63 ± 0.04	0.03 ± 0.01	0.08 ± 0.03	0.27 ± 0.02	0.73 ± 0.13	0.08 ± 0.07	0.19 ± 0.16	0.37 ± 0.04
	10	0.33 ± 0.01	0.10 ± 0.04	0.14 ± 0.05	0.38 ± 0.02	0.57 ± 0.02	0.19 ± 0.04	0.29 ± 0.07	0.67 ± 0.01
	50	0.21 ± 0.05	0.17 ± 0.05	0.22 ± 0.08	0.34 ± 0.07	0.43 ± 0.06	0.28 ± 0.04	0.35 ± 0.03	0.79 ± 0.05
saturated	0.1	0.81 ± 0.05	0.03 ± 0.03	0.12 ± 0.10	0.12 ± 0.04	0.58 ± 0.04	0.05 ± 0.01	0.30 ± 0.13	0.20 ± 0.05
	1	0.67 ± 0.04	0.06 ± 0.01	0.18 ± 0.01	0.22 ± 0.06	0.65 ± 0.10	0.06 ± 0.03	0.17 ± 0.11	0.33 ± 0.04
	10	0.30 ± 0.01	0.10 ± 0.02	0.14 ± 0.03	0.43 ± 0.01	0.61 ± 0.02	0.17 ± 0.03	0.25 ± 0.05	0.70 ± 0.01
	50	0.22 ± 0.01	0.36 ± 0.04	0.46 ± 0.05	0.32 ± 0.06	0.41 ± 0.08	0.11 ± 0.03	0.14 ± 0.03	0.78 ± 0.01
two-way ANOVA[b]	saturation	0.434 ns	0.004 **	0.008 **	0.565 ns	0.192 ns	0.018 *	0.250 ns	0.434 ns
	IS	0.000 ***	0.000 ***	0.000 ***	0.000 ***	0.256 ns	0.001 ***	0.587 ns	0.000 ***
	interaction	0.449 ns	0.004 **	0.034 *	0.512 n.s.	0.618 ns	0.037 *	0.539 ns	0.449 n.s.

[a]The symbol W indicate the amount of colloids released in the water, and M for the colloids associated with the sand. The subscript numbers indicate the phase of the experiment, and the subscript letters indicate if the amount of colloids are expressed as a fraction of the amount of total colloids applied (subscript T) or the amount retained during phase 1 (subscript R). [b]Two-way ANOVA: main effects of saturation and IS, and the interaction effect between saturation and IS; ns: no significant difference ($p > 0.05$); *: $0.01 < p < 0.05$; **: $0.001 < p < 0.01$; ***: $p < 0.001$.

coefficients (D). The Cl^- concentration in the tracer breakthrough experiments was analyzed with ion chromatography (Dionex ICS-2000 with Ion Pac AS18 column, Dionex, Sunnyvale, CA) and the BTCs were fitted with a steady-state equilibrium convective−dispersive transport equation using CXTFIT 2.1. Details regarding the tracer test are provided in the SI S5. The values of v and D was determined to be 1.2 cm min^{-1} and 0.11 cm^2 min^{-1} for saturated conditions, and 3.5 cm min^{-1} and 1.89 cm^2 min^{-1} for unsaturated conditions, respectively. Because the velocities used for this study are comparably greater than what is expected for groundwater transport, the hydrodynamic forces in the system create conditions that are less favorable for retention (smaller regions of stagnant flow) and increase the likelihood for mechanical detachment of retained colloids from strong applied torque.[19,48] Hence, colloid retention is expected to be greater under slower flow velocities, and the results reported should be considered conservative representation of natural occurring systems with regard to colloid deposition. Steady-state colloid deposition rate coefficients (k_d) for the BTC of phase 1 were calculated as described in SI S5.[15]

Retention by secondary minima, pore straining, and primary minima are determined as follows. Reversible secondary minima retention (W_{T2}) was determined as the fraction of the total applied colloids eluted from the column in phase 2 (i.e., after flushing the system with DI water). Retention by pore straining (W_{T3}) was the fraction of the total applied colloids recovered after dissecting the column, whereby pore restrictions were eliminated and strained colloids liberated. Lastly, irreversible primary minima retention (M_{T3}) was calculated from mass balance of the total amount of colloids added in phase 1, and the amount recovered in the effluent and in the column dissection. Corroboration of the presence of irreversibly attached colloids on media grains was obtained from images of the sand surface after washing (SI Figure S7). Two-way analysis of variance (ANOVA) was employed to compare the fraction of colloids retained by each retention mechanism for each set of experimental conditions. The independent and coupled (interaction) effects of water saturation and IS were analyzed, and significance of the effect was determined by p-values for each set of data.

Calculation of DLVO Interaction Energy and Attachment Efficiencies. Colloid-colloid and colloid-sand interaction energy profiles were calculated using DLVO theory as the sum of retarded van der Waals and electrostatic (calculated from linear superposition approximation) interaction energies. Detailed equations are provided in SI S7. DLVO energy profiles are used in later sections to explain observed trends in colloid retention at primary and secondary energy minima.

Additionally, attachment efficiency (α) was calculated according to previous methods[22,27,49] to determine the likelihood of colloid collisions resulting in aggregation or attachment. The method by Shen et al.[22] was used for determining the attachment efficiency of colloid to the media surface, whereas the method by Marmur[49] was used to determine the attachment efficiency for colloid aggregation. Details of the calculations are given in SI S7.

RESULTS

Colloid Retention and Release at Steady Ionic Strength (Phase 1). Observed BTCs for phases 1 and 2 in both saturated and unsaturated media are shown in Figure 1. In phase 1, colloids were injected and then flushed with a colloid-free background solution of matching IS. Minor perturbations to phase 1 BTCs (as indicated by red arrows in Figure 1) are possibly a result of flow disturbance during changing the influent solutions. Colloids arrived similarly at the outlet in the unsaturated conditions compared with the saturated conditions, which is consistent with chloride BTCs (SI Figure S5). Consistent with previous studies,[1,30,50] colloid effluent recovery decreased significantly from 81% to 21% of the applied colloids with increasing IS (Figure 1 and W_{T1} values in Table 1). The

difference in colloid mass retained as a function of the total amount applied (M_{T1} in Table 1) between saturated and unsaturated flow at the same IS was not significant.

Although similar amounts of colloids were retained in phase 1 (W_{T1}) for saturated and unsaturated conditions at equivalent IS, deposition rate coefficients (k_d) in unsaturated media were significantly greater than the k_d values for saturated conditions at all IS levels, as presented in Figure 2, despite an over 3-fold

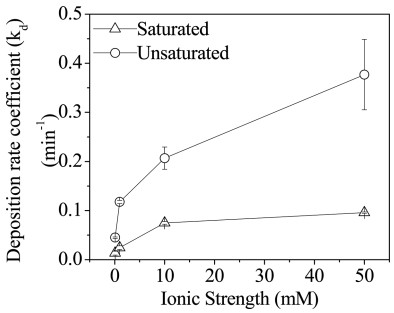

Figure 2. Colloid deposition rate coefficients in saturated and unsaturated media.

increase in pore water velocity in unsaturated columns. This observation conflicts with reduced retention expected at high flow velocities, as is the case in unsaturated experiments, due to increased bulk flow advection and hydrodynamic drag force, as well as decreased low-flow zone.[4,19,40,48] Nonetheless, the presence of an air phase provided additional retention sites such as AWS interfaces and low velocity zones that could retain more colloids effectively, thus outperforming the velocity effect and resulting in larger k_d values under unsaturated conditions. This observation is reinforced with visual data in the following, which indicate that at the pore-scale colloid retention in sites unique to unsaturated systems becomes more efficient with increasing IS (Figure 3).

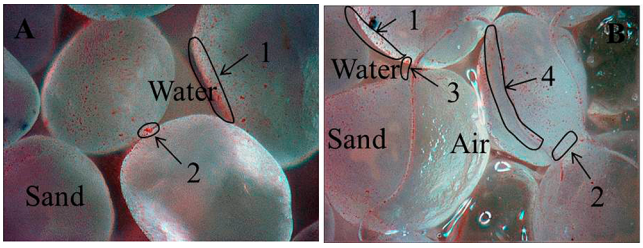

Figure 3. Observed colloid retention sites in saturated (A) and unsaturated (B) sand columns at 50 mM ionic strength and at the end of 20 mL colloid injection: 1. solid-water interface (SWI); 2. grain-to-grain contact; 3. air–water interface (AWI); 4. air–water–solid (AWS) interface.

Retention Sites. From pore-scale images collected during column experiments, four distinct and well-documented mechanisms were identified to contribute to colloid retention. Two retention mechanisms participating in both saturated and unsaturated media were colloid attachment at the solid-water interface (SWI) (site 1) and straining at grain-to-grain contacts (site 2) in Figure 3. In unsaturated media, two additional retention sites can be observed, including retention at the air–water interface (AWI) (site 3) and the air–water–solid (AWS) interface (site 4) in Figure 3. Visual data confirm retention in the air-associated interfaces, which are the sites associated with capillary forces and low velocity zones. However, due to the limited number of pores visualized here, the importance of retention at various interfaces cannot be quantified. Rather, these data were used to qualitatively corroborate colloid retention in air-associated interfaces and on grains after column dissection.

Colloid Release by Ionic Strength Reduction (Phase 2). Phase 2 was defined as a chemical transient event that sharply reduced the IS by DI water injection. In this phase, those experiments of initially higher IS (in phase 1) released more colloids in the effluent both as fraction of the total amount of colloids applied (see second BTC in Figure 1 and W_{T2} in Table 1), as well as a fraction of the amount of colloids retained in phase 1 (W_{R2} in Table 1). For low IS (i.e., 0.1, 1, and 10 mM), colloid released (W_{R2}) ranged between 8 and 18% of the colloids retained in phase 1 (i.e., the first BTC) at both levels of water saturation. Similarities in detachment processes at low IS between saturated and unsaturated conditions are evident in the resemblances in shape and size of the second BTCs at low IS levels (Figure 1A–C and E–G). However, at the highest IS condition (50 mM) 46% of the colloids retained in phase 1 were released in the saturated experiments when the IS was reduced (Figure 1D and W_{R2} in Table 1), whereas only 22% was released for unsaturated conditions (Figure 1H and W_{R2} Table 1). In addition, pronounced differences in detachment processes are evident in the shape of the second BTC of the high IS experiments. The BTCs of Figure 1D and H suggest that colloids in the saturated column became highly concentrated before being eluted (C/C_0 >1). This effect is discussed in detail in the Discussion section.

Colloid Retention Profiles. Colloids recovered by column dissection, which removed the structure of porous medium, were classified as strained. Recovery of strained colloids ranged from 12% of the total amount applied for the low IS to 43% for intermediate IS (W_{T3} in Table 1) in all experiments. At high IS, 32–34% of colloids were strained. Colloid retention by straining increased significantly with increasing IS when expressed as a fraction of the amount of colloids applied (W_{T3} in Table 1). However, when expressed as a fraction of the colloids retained in the column after phase 1 (W_{R3} in Table 1) straining was independent of IS or water saturation degree.

The depth profiles of colloids retained by straining are shown in SI Figure S6. As has been often observed, colloid retention is greatest at the column inlet (depths near 0 cm), and is more pronounced for unsaturated conditions. Generally, colloids are retained in greater quantities with increasing initial IS levels (W_{R3} in Table 1). This is in agreement with the total amount of colloids retained at the end of phase 1 (W_{T1} in Table 1), which was highly dependent on IS.

Irreversible Colloid Retention. The amount of colloids classified as irreversibly attached to the sand surface was calculated by mass balance of the colloids initially added, minus the colloids eluted in the effluent of phases 1 and 2, and those recovered by column dissection. Although it is aknowledged that estimating primary minimum retention in this manner is subject to inaccuracy from experimental error, mass balance of experiments that experienced minimal retention approached 100%, so we consider the potential error acceptably low. Visual evidence of colloids present on the sand corroborates primary minimum retention (SI Figure S7). The amount of colloids retained by primary minimum interactions increased significantly with IS and was greater for unsaturated than saturated conditions when expressed as a fraction of the total amount

dx.doi.org/10.1021/es400288c | Environ. Sci. Technol. 2013, 47, 8256–8264

applied (M_{T3} in Table 1). When expressed as a fraction of the amount of colloids in the column at the end of phase 1, there were no statistically significant differences either with moisture content or IS (M_{R3} in Table 1).

Interaction Energy Profiles and Attachment Efficiency. The EM and ζ-potential of the colloids and the quartz sand fragments indicated that negative surface charge was maintained for all the conditions investigated, and predictably became less negative with increasing IS (SI Table S1). In general, DLVO energy profiles are characterized by large primary minima wells at separation distances <1 nm, large energy barriers of 10^3 kT magnitude, and shallow secondary minima wells at distances <500 nm (SI Figure S8 and Table S3). An increase in IS resulted in deeper secondary minimum wells and shorter energy barrier heights. Of the tested conditions, only the profiles at the lowest IS (DI water) did not possess secondary minimum wells (SI Figure S8).

The attachment efficiency (α) for both colloid−colloid and colloid-SWI interactions are shown in SI Table S3. As expected, the α values increased with IS, as a result of increasing secondary minimum depths. Because of the large energy barriers, the α for the primary minimum is zero. The α value for colloid deposition is calculated based on the DLVO energy of colloid interacting with homogeneous smooth quartz surface, thus excluding the role of surface charge heterogeneity. When IS increased to 50 mM, the α value of colloid-SWI reached 1, whereas the α value for colloid aggregation became 0.696. In agreement with the colloid size measurement (SI Figure S1), colloid aggregation is expected to be minimal at lower IS levels due to low α values, but become important at 50 mM IS (SI Table S3).

DISCUSSION

Colloid Transport and Deposition Rate Coefficients. The BTCs in Figure 1 indicate that for all the conditions tested, the available retention sites in the porous media did not become saturated. One factor that may be responsible for this observation is the high bulk flow velocity, which minimizes the possibility of colloids to cross streamlines and diffuse toward retention sites near boundaries. This is evident in the BTC peak values of phase 1, which only reached a maximum of approximately 0.8 C/C_0 for the two lower IS conditions; while the two higher IS conditions reached a maximum of 0.4 C/C_0. Conversely, the BTCs of phase 2 changed shape with both IS and water saturation level. The peaks for the low IS conditions in phase 2 are minimal, since most of the colloids that remained within the column were either strained or held in primary minima. Of particular importance are the results BTCs of phase 2 at the highest IS level (50 mM), which are narrow and tall for saturated conditions, but wide and short for unsaturated conditions. This drastic change in shape indicates that: first, the peak of the phase 2 BTC is broadened by a factor of 3, as the PV of the unsaturated media is approximately 30% of the saturated PV; second, given the similar release time, the lower release colloid mass under unsaturated conditions (Table 1) demonstrated more efficient colloid capture at the unsaturated retention sites.

Since flow pattern is independent of IS, the increase in k_d with IS (Figure 2) is attributed to changes in attachment efficiency, which increased with increasing IS (SI Table S3). Deposition rates for unsaturated media were significantly greater than for saturated media (Figure 2). This trend holds true despite the near 3-fold increase in pore water velocity in unsaturated conditions, compared to conditions of full saturation, which is expected to produce minimal regions of low-flow or hydrodynamic isolation where colloids can become immobilized.[4,19] Thus, it would be expected that, from a hydrodynamic perspective, colloids traveling in unsaturated media at high velocities should be subject to lower retention than in saturated media at lower velocities. However, the opposite effect was observed, suggesting that colloid retention was dominated by interactions with the identified retention sites (e.g., the AWS interfaces) as shown in Figure 3. As such, it is expected that retention at sites interfacing the air are likely highly efficient and act quickly to remove colloids from the bulk fluid, thus resulting in higher k_d in unsaturated than saturated conditions.

Reversible Colloid Retention by Secondary Minimum Interactions. The release of colloids by chemical transients (as produced by phase 2 of the transport experiments) are here attributed to the elimination of secondary energy minimum wells. Because secondary minimum interactions are nonexistent in DI water (SI Table S3), any colloids that were loosely retained by secondary minimum interactions at nonzero IS conditions in phase 1 were released when IS was reduced to that of DI. This produced the second BTC in Figure 1. This trend is in agreement with numerous previous studies.[22,26−28,41,47,52] The depth of the secondary minimum well (or α values) is directly correlated to solution IS, as is evident in SI Figure S8 and Table S3. Thus, the quantity of colloids released when attractive secondary minimum interactions were diminished was correlated to the well depth at initial IS conditions of phase 1.

Colloid Retention by Straining. The proportion of colloids retained by straining was attributed to the structural restrictions of the porous medium and the geometry of the liquid phase through which the colloids traveled. For saturated systems, structural restrictions are expected to occur when colloid-grain ratios are large,[12,18,53] at small regions near grain-to-grain contacts,[3,54] as well as in surface crevices where surface roughness is larger than colloid radius and flow velocities are low. For unsaturated systems, the water flow is further restricted by the presence of air pockets to thin water film enveloping grain surface, pendular rings near the grain-to-grain contacts, and the AWS interfaces.[12,13] Thus, the depth-dependent colloid retention (SI Figure S6) is more pronounced in unsaturated conditions. It was noted that the colloid-grain ratios are approximately 0.004−0.005, in agreement with the reported threshold ratio of 0.0017−0.005[12,35,54] when straining becomes important. The measured colloid hydrodynamic diameters remained relatively unchanged over the experimental period, and colloids were slightly aggregated in 50 mM NaCl solution (SI Figure S1). It is understood that aggregate size measurements made in batch are expected to underestimate the size of aggregates forming in the column, where flow-induced aggregation or orthokinetic aggregation occurs.[55−57] Here, our results indicate that the proportion of colloids retained by straining processes greatly exceeded that by secondary or primary minimum interactions.

Irreversible Colloid Retention by Primary Minimum Interactions. We propose that capillary forces are responsible for colloid interactions at the primary minimum with the grain surface in the presence of high energy barriers (SI Figure S8). These capillary forces arise at the AWS interface in unsaturated conditions, which has been alluded to previously.[31,58−60] The energy associated with this force has been calculated to be at

least 1 order of magnitude larger than energy barriers encountered under environmental conditions, thereby providing the necessary force to push the colloids through the energy barrier in unsaturated conditions.[31] Additionally, primary minima attachment can result from surface charge heterogeneities on the sand surface, despite acid-cleaning treatments, as reported by Li et al.[61]

With regard to the difference in primary minimum retention observed at 50 mM IS between the two water saturations investigated, we hypothesize that it can then be explained by the capillary forces operative under unsaturated conditions. For unsaturated conditions, favorable microsites on the sand surface as well as capillary forces, which push the colloids through the large energy barrier and into the primary minimum well,[32] promote retention by primary minimum interactions. For saturated conditions, only favorable microsites on the sand promote primary minimum interactions. Therefore, a lesser proportion of colloids are retained by irreversible primary minimum interactions in saturated than unsaturated conditions.

In the photographs of the gain surfaces after column dissection (SI Figure S7), it is evident that at 50 mM IS more colloids remain on the sand surface in unsaturated experiments (SI Figure S7D) than in saturated experiments (SI Figure S7E). This is consistent with the M_{T3} values at 50 mM IS (Table 1). Careful examination of SI Figure S7 reveals that colloids are arranged in "strings" for the sand grains recovered from unsaturated experiments. Here we propose that the string arrangement is due to colloid pinning at AWS contact lines, which pushed them into the primary minimum. However, for the sand from saturated experiments, colloids are found bunched up in small aggregates in the grain cavities. It is possible that the colloids in the cavities were hydrodynamically shielded from bulk fluid shear, thus having greater likelihood of crossing streamlines to be attracted to favorable microsites.

In summary, straining was found to be the largest contributor toward colloid retention for all tested conditions with an enhanced effect under unsaturated conditions due to the more restrictive pore space. Reversible retention by secondary minimum was found to be the second most important mechanism in saturated conditions due to the unconfined availability for interaction with the SWI. Conversely, irreversible retention by primary minimum was the second most important retention mechanism in unsaturated conditions due to association of the colloids with AWS interfaces. Capillary forces at the AWS were deemed strong enough to help colloids overcome repulsive energy barriers and affect primary minimum interactions with the sand surface. The knowledge gained in this study regarding identification of colloid retention mechanisms in a porous medium of simple properties, and quantification of the relative importance of these mechanisms should help improve transport models that capture emergent transport processes in complex porous media, such as natural soils.

■ ASSOCIATED CONTENT

Supporting Information

Supporting Information contains the following: S1. Electrophoretic mobility and hydrodynamic diameter measurements; S2. Unsaturated experimental setup; S3. Experimental protocol flowchart; S4. Chloride concentration changes in phase 2; S5. Transport model and tracer experiments; S6. Column dissection experiments; S7. DLVO energy calculations and attachment efficiency. This material is available free of charge via the Internet at http://pubs.acs.org.

■ AUTHOR INFORMATION

Corresponding Author

*(Y.Z.) Phone: +86 21 65985811; e-mail: zhangyalei@tongji.edu.cn. (T.S.S.) Phone: +1 607 255 2489; e-mail: tss1@cornell.edu.

Notes

The authors declare no competing financial interest.

■ ACKNOWLEDGMENTS

We thank Douglas Caveney for help with constructing the flow chambers, and Shree Giri for help with chemical analysis. This research was supported by the Chinese Scholarship Council for Wenjing Sang, USDA-National Research Initiative (Project 2005-03929 and 2008-35102-04462), the National Science Foundation (Project 2006-0635954), the National Natural Science Foundation of China (Project 51138009), and the National Key Technology Research and Development Program funded by the Ministry of Science and Technology of China (Project 2012BAJ25B02). Verónica L. Morales was supported by a Marie Curie Action International Incoming Fellowship (FP7-PEOPLE-2012-SoilArchnAg).

■ REFERENCES

(1) de Jonge, L. W.; Kjaergaard, C.; Moldrup, P. Colloids and colloid-facilitated transport of contaminants in soils: An introduction. *Vadose Zone J.* **2004**, *3* (2), 321−325.

(2) McCarthy, J. F.; McKay, L. D. Colloid transport in the subsurface. *Vadose Zone J.* **2004**, *3* (2), 326−337.

(3) Torkzaban, S.; Tazehkand, S. S.; Walker, S. L.; Bradford, S. A. Transport and fate of bacteria in porous media: Coupled effects of chemical conditions and pore space geometry. *Water Resour. Res.* **2008**, *44* (4).

(4) Bradford, S. A.; Torkzaban, S.; Walker, S. L. Coupling of physical and chemical mechanisms of colloid straining in saturated porous media. *Water Res.* **2007**, *41* (13), 3012−3024.

(5) Bian, S.-W.; Mudunkotuwa, I. A.; Rupasinghe, T.; Grassian, V. H. Aggregation and dissolution of 4 nm ZnO nanoparticles in aqueous environments: Influence of pH, ionic strength, size, and adsorption of humic acid. *Langmuir* **2011**, *27* (10), 6059−6068.

(6) Torkzaban, S.; Hassanizadeh, S. M.; Schijven, J. F.; van den Berg, H. Role of air-water interfaces on retention of viruses under unsaturated conditions. *Water Resour. Res.* **2006**, *42* (12).

(7) Torkzaban, S.; Hassanizadeh, S. M.; Schijven, J. F.; de Bruin, H. A. M.; Husman, A. Virus transport in saturated and unsaturated sand columns. *Vadose Zone J.* **2006**, *5* (3), 877−885.

(8) Chowdhury, I.; Cwiertny, D. M.; Walker, S. L. Combined factors influencing the aggregation and deposition of nano-TiO_2 in the presence of humic acid and bacteria. *Environ. Sci. Technol.* **2012**, *46* (13), 6968−6976.

(9) Crist, J. T.; McCarthy, J. F.; Zevi, Y.; Baveye, P.; Throop, J. A.; Steenhuis, T. S. Pore-scale visualization of colloid transport and retention in partly saturated porous media. *Vadose Zone J.* **2004**, *3* (2), 444−450.

(10) Crist, J. T.; Zevi, Y.; McCarthy, J. F.; Throop, J. A.; Steenhuis, T. S. Transport and retention mechanisms of colloids in partially saturated porous media. *Vadose Zone J.* **2005**, *4* (1), 184−195.

(11) Wan, J.; Tokunaga, T. K. Partitioning of clay colloids at air-water interfaces. *J. Colloid Interface Sci.* **2002**, *247* (1), 54−61.

(12) Bradford, S. A.; Simunek, J.; Bettahar, M.; van Genuchten, M. T.; Yates, S. R. Significance of straining in colloid deposition: Evidence and implications. *Water Resour. Res.* **2006**, *42* (12).

(13) Bradford, S. A.; Torkzaban, S. Colloid transport and retention in unsaturated porous media: A review of interface-, collector-, and pore-scale processes and models. *Vadose Zone J.* **2008**, *7* (2), 667−681.
(14) Morales, V. L.; Gao, B.; Steenhuis, T. S. Grain Surface-roughness effects on colloidal retention in the vadose zone. *Vadose Zone J.* **2009**, *8* (1), 11−20.
(15) Zhang, W.; Morales, V. L.; Cakmak, M. E.; Salvucci, A. E.; Geohring, L. D.; Hay, A. G.; Parlange, J.-Y.; Steenhuis, T. S. Colloid transport and retention in unsaturated porous media: Effect of colloid input concentration. *Environ. Sci. Technol.* **2010**, *44* (13), 4965−4972.
(16) Ryan, J. N.; Illangasekare, T. H.; Litaor, M. I.; Shannon, R. Particle and plutonium mobilization in macroporous soils during rainfall simulations. *Environ. Sci. Technol.* **1998**, *32* (4), 476−482.
(17) Shang, J.; Flury, M.; Chen, G.; Zhuang, J. Impact of flow rate, water content, and capillary forces on in situ colloid mobilization during infiltration in unsaturated sediments. *Water Resour. Res.* **2008**, *44* (6), W06411.
(18) Torkzaban, S.; Bradford, S. A.; van Genuchten, M. T.; Walker, S. L. Colloid transport in unsaturated porous media: The role of water content and ionic strength on particle straining. *J. Contam. Hydrol.* **2008**, *96* (1−4), 113−127.
(19) Torkzaban, S.; Bradford, S. A.; Walker, S. L. Resolving the coupled effects of hydrodynamics and DLVO forces on colloid attachment in porous media. *Langmuir* **2007**, *23* (19), 9652−9660.
(20) Tosco, T.; Bosch, J.; Meckenstock, R. U.; Sethi, R. Transport of ferrihydrite nanoparticles in saturated porous media: Role of ionic strength and flow rate. *Environ. Sci. Technol.* **2012**, *46* (7), 4008−4015.
(21) Bhattacharjee, S.; Ryan, J. N.; Elimelech, M. Virus transport in physically and geochemically heterogeneous subsurface porous media. *J. Contam. Hydrol.* **2002**, *57* (3−4), 161−187.
(22) Shen, C.; Li, B.; Huang, Y.; Jin, Y. Kinetics of coupled primary- and secondary-minimum deposition of colloids under unfavorable chemical conditions. *Environ. Sci. Technol.* **2007**, *41* (20), 6976−6982.
(23) Ma, H.; Pazmino, E. F.; Johnson, W. P. Gravitational settling effects on unit cell predictions of colloidal retention in porous media in the absence of energy barriers. *Environ. Sci. Technol.* **2011**, *45* (19), 8306−8312.
(24) Chen, L.; Tian, Y.; Cao, C.-q.; Zhang, J.; Li, Z.-n. Interaction energy evaluation of soluble microbial products (SMP) on different membrane surfaces: Role of the reconstructed membrane topology. *Water Res.* **2012**, *46* (8), 2693−2704.
(25) Johnson, W. P.; Tong, M.; Li, X. On colloid retention in saturated porous media in the presence of energy barriers: The failure of α, and opportunities to predict η. *Water Resour. Res.* **2007**, *43* (12), W12S13.
(26) Tufenkji, N.; Elimelech, M. Breakdown of colloid filtration theory: Role of the secondary energy minimum and surface charge heterogeneities. *Langmuir* **2005**, *21* (3), 841−852.
(27) Hahn, M. W.; Abadzic, D.; O'Melia, C. R. Aquasols: On the role of secondary minima. *Environ. Sci. Technol.* **2004**, *38* (22), 5915−5924.
(28) Redman, J. A.; Walker, S. L.; Elimelech, M. Bacterial adhesion and transport in porous media: Role of the secondary energy minimum. *Environ. Sci. Technol.* **2004**, *38* (6), 1777−1785.
(29) Jin, Y.; Chu, Y.; Li, Y. Virus removal and transport in saturated and unsaturated sand columns. *J. Contam. Hydrol.* **2000**, *43* (2), 111−128.
(30) Saiers, J. E.; Lenhart, J. J. Ionic-strength effects on colloid transport and interfacial reactions in partially saturated porous media. *Water Resour. Res.* **2003**, *39* (9), 1256.
(31) Gao, B.; Steenhuis, T. S.; Zevi, Y.; Morales, V. L.; Nieber, J. L.; Richards, B. K.; McCarthy, J. F.; Parlange, J. Y. Capillary retention of colloids in unsaturated porous media. *Water Resour. Res.* **2008**, *44* (4), W04504.
(32) Zevi, Y.; Gao, B.; Zhang, W.; Morales, V. L.; Ekrem Cakmak, M.; Medrano, E. A.; Sang, W.; Steenhuis, T. S. Colloid retention at the meniscus-wall contact line in an open microchannel. *Water Res.* **2012**, *46* (2), 295−306.
(33) Matthess, G.; Pekdeger, A. *Survival and Transport of Pathogenic Bacteria and Viruses in Goundwater*; John Wiley and Sons: New York, 1985.
(34) Li, X.; Scheibe, T. D.; Johnson, W. P. Apparent decreases in colloid deposition rate coefficients with distance of transport under unfavorable deposition conditions: A general phenomenon. *Environ. Sci. Technol.* **2004**, *38* (21), 5616−5625.
(35) Bradford, S. A.; Yates, S. R.; Bettahar, M.; Simunek, J. Physical factors affecting the transport and fate of colloids in saturated porous media. *Water Resour. Res.* **2002**, *38* (12), 1327−1338.
(36) Bradford, S. A.; Simunek, J.; Bettahar, M.; van Genuchten, M. T.; Yates, S. R. Modeling colloid attachment, straining, and exclusion in saturated porous media. *Environ. Sci. Technol.* **2003**, *37* (10), 2242−2250.
(37) Foppen, J. W. A.; Mporokoso, A.; Schijven, J. F. Determining straining of *Escherichia coli* from breakthrough curves. *J. Contam. Hydrol.* **2005**, *76* (3−4), 191−210.
(38) Auset, M.; Keller, A. A. Pore-scale visualization of colloid straining and filtration in saturated porous media using micromodels. *Water Resour. Res.* **2006**, *42* (12), W12S02.
(39) Kretzschmar, R.; Barmettler, K.; Grolimund, D.; Yan, Y.-d.; Borkovec, M.; Sticher, H. Experimental determination of colloid deposition rates and collision efficiencies in natural porous media. *Water Resour. Res.* **1997**, *33* (5), 1129−1137.
(40) Li, X.; Zhang, P.; Lin, C. L.; Johnson, W. P. Role of hydrodynamic drag on microsphere deposition and re-entrainment in porous media under unfavorable conditions. *Environ. Sci. Technol.* **2005**, *39* (11), 4012−4020.
(41) Tufenkji, N.; Elimelech, M. Deviation from the classical colloid filtration theory in the presence of repulsive DLVO interactions. *Langmuir* **2004**, *20* (25), 10818−10828.
(42) Bradford, S. A.; Torkzaban, S.; Shapiro, A. A theoretical analysis of colloid attachment and straining in chemically heterogeneous porous media. *Langmuir* **2013**, In press.
(43) Kuznar, Z. A.; Elimelech, M. Direct microscopic observation of particle deposition in porous media: Role of the secondary energy minimum. *Colloids Surf., A* **2007**, *294* (1−3), 156−162.
(44) Litton, G. M.; Olson, T. M. Colloid deposition rates on silica bed media and artifacts related to collector surface preparation methods. *Environ. Sci. Technol.* **1993**, *27* (1), 185−193.
(45) Ottewill, R. H.; Shaw, J. N. Electrophoretic studies on polystyrene latices. *J. Electroanal. Chem.* **1972**, *37* (1), 133−142.
(46) O'Brien, R. W.; Hunter, R. J. The electrophoretic mobility of large colloidal particles. *Can. J. Chem.* **1981**, *59* (13), 1878−1887.
(47) Franchi, A.; O'Melia, C. R. Effects of natural organic matter and solution chemistry on the deposition and reentrainment of colloids in porous media. *Environ. Sci. Technol.* **2003**, *37* (6), 1122−1129.
(48) Bradford, S. A.; Torkzaban, S.; Wiegmann, A. Pore-scale simulations to determine the applied hydrodynamic torque and colloid immobilization. *Vadose Zone J.* **2011**, *10* (1), 252−261.
(49) Marmur, A. A kinetic theory approach to primary and secondary minimum coagulations and their combination. *J. Colloid Interface Sci.* **1979**, *72* (1), 41−48.
(50) Liu, D.; Johnson, P. R.; Elimelech, M. Colloid deposition dynamics in flow-through porous media: Role of electrolyte concentration. *Environ. Sci. Technol.* **1995**, *29* (12), 2963−2973.
(51) Hahn, M. W.; O'Melia, C. R. Deposition and reentrainment of Brownian particles in porous media under unfavorable chemical conditions: Some concepts and applications. *Environ. Sci. Technol.* **2004**, *38* (1), 210−220.
(52) Shen, C.; Li, B.; Wang, C.; Huang, Y.; Jin, Y. Surface roughness effect on deposition of nano- and micro-sized colloids in saturated columns at different solution ionic strengths. *Vadose Zone J.* **2011**, *10* (3), 1071−1081.
(53) Bradford, S. A.; Simunek, J.; Bettahar, M.; Tadassa, Y. F.; van Genuchten, M. T.; Yates, S. R. Straining of colloids at textural interfaces. *Water Resour. Res.* **2005**, *41* (10), W10404.

(54) Johnson, W. P.; Li, X.; Yal, G. Colloid retention in porous media: Mechanistic confirmation of wedging and retention in zones of flow stagnation. *Environ. Sci. Technol.* **2007**, *41* (4), 1279−1287.
(55) Ramachandran, V.; Fogler, H. S. Multilayer deposition of stable colloidal particles during flow within cylindrical pores. *Langmuir* **1998**, *14* (16), 4435−4444.
(56) Bradford, S. A.; Simunek, J.; Walker, S. L. Transport and straining of *E. coli* O157:H7 in saturated porous media. *Water Resour. Res.* **2006**, *42* (12), W12S12.
(57) Tong, M. P.; Ma, H. L.; Johnson, W. P. Funneling of flow into grain-to-grain contacts drives colloid-colloid aggregation in the presence of an energy barrier. *Environ. Sci. Technol.* **2008**, *42* (8), 2826−2832.
(58) Danov, K. D.; Kralchevsky, P. A. Electric forces induced by a charged colloid particle attached to the water-nonpolar fluid interface. *J. Colloid Interface Sci.* **2006**, *298* (1), 213−231.
(59) Danov, K. D.; Kralchevsky, P. A.; Naydenov, B. N.; Brenn, G. Interactions between particles with an undulated contact line at a fluid interface: Capillary multipoles of arbitrary order. *J. Colloid Interface Sci.* **2005**, *287* (1), 121−134.
(60) Kralchevsky, P. A.; Denkov, N. D. Capillary forces and structuring in layers of colloid particles. *Curr. Opin. Colloid Interface Sci.* **2001**, *6* (4), 383−401.
(61) Li, Y. S.; Wang, Y. G.; Pennell, K. D.; Abriola, L. M. Investigation of the transport and deposition of fullerene (C60) nanoparticles in quartz sands under varying flow conditions. *Environ. Sci. Technol.* **2008**, *42* (19), 7174−7180.